Title: Cascading influence of inorganic nitrogen sources on DOM production, composition, lability and microbial community structure in the open ocean.
Running Title: Nitrogen source effects on marine DOM and microbes
Authors: SJ Goldberg[#], CE Nelson*, DA Viviani, CN Shulse[‡] and MJ Church[§]

Stuart J. Goldberg, Center for Microbial Oceanography: Research and Education, Department of Oceanography, School of Ocean and Earth Science and Technology, 1950 East West Road, University of Hawai'i at Mānoa, Honolulu, Hawai'i, USA 96822.
[#]Current address: Habitat Conservation Division, NOAA Fisheries, Pacific Islands Regional Office, Inouye Regional Center, 1845 Wasp Blvd., Honolulu, HI 96818

Craig E. Nelson, Center for Microbial Oceanography: Research and Education, Department of Oceanography and Sea Grant College Program, School of Ocean and Earth Science and Technology, 1950 East West Road, University of Hawai'i at Mānoa, Honolulu, Hawai'i, USA 96822. *Author to whom correspondence should be addressed.
Telephone: +1 808-956-0566. Fax: +1 808-956-0581. Email: craig.nelson@hawaii.edu

Donn A. Viviani, Center for Microbial Oceanography: Research and Education, Department of Oceanography, School of Ocean and Earth Science and Technology, 1950 East West Road, University of Hawai'i at Mānoa, Honolulu, Hawai'i, USA 96822.

Christine N. Shulse, Center for Microbial Oceanography: Research and Education, Department of Oceanography, School of Ocean and Earth Science and Technology, 1950 East West Road, University of Hawai'i at Mānoa, Honolulu, Hawai'i, USA 96822.
[‡]Current contact information: Department of Energy Joint Genome Institute, 2800 Mitchell Drive, Walnut Creek, CA, USA 94598.

Matthew J. Church, Center for Microbial Oceanography: Research and Education, Department of Oceanography, School of Ocean and Earth Science and Technology, 1950 East West Road, University of Hawai'i at Mānoa, Honolulu, Hawai'i, USA 96822.
[§]Current contact information: Flathead Lake Biological Station, University of Montana, 32125 Bio Station Lane, Polson, MT 59860-6815

Conflict of Interest Statement: The authors declare no conflict of interest.
Support: This work was supported by grants from the National Science Foundation (NSF) (OCE-1241263 and OCE-1260164 to MJC, OCE-1538428 to CEN), with additional support from the Simons Collaboration on Ocean Processes and Ecology (SCOPE to MJC) and the NSF Center for Microbial Oceanography: Research and Education (C-MORE, NSF EF-0424599).

This article has been accepted for publication and undergone full peer review but has not been through the copyediting, typesetting, pagination and proofreading process which may lead to differences between this version and the Version of Record. Please cite this article as an 'Accepted Article', doi: 10.1111/1462-2920.13825

Originality-Significance Statement:

This work demonstrates that inorganic nitrogen sources can differentially influence the composition and lability of microbially-produced dissolved organic matter (DOM) with subsequent effects on heterotrophic community metabolism and microbial phylogenetic structure over weekly timescales in the open ocean.

Summary

Nitrogen frequently limits oceanic photosynthesis and the availability of inorganic nitrogen sources in the surface oceans is shifting with global change. We evaluated the potential for abrupt increases in inorganic N sources to induce cascading effects on DOM and microbial communities in the surface ocean. We collected water from 5 m depth in the central North Pacific and amended duplicate 20 L polycarbonate carboys with nitrate or ammonium, tracking planktonic carbon fixation, DOM production, DOM composition and microbial community structure responses over 1 week relative to controls. Both nitrogen sources stimulated bulk phytoplankton, bacterial and DOM production and enriched *Synechococcus* and Flavobacteriaceae; ammonium enriched for oligotrophic Actinobacteria OM1 and Gammaproteobacteria KI89A clades while nitrate enriched Gammaproteobacteria SAR86, SAR92 and OM60 clades. DOM resulting from both N enrichments was more labile and stimulated growth of copiotrophic Gammaproteobacteria (Alteromonadaceae and Oceanospirillaceae) and Alphaproteobacteria (Rhodobacteraceae and Hyphomonadaceae) in weeklong dark incubations relative to controls. Our study illustrates how nitrogen pulses may have direct and cascading effects on DOM composition and microbial community dynamics in the open ocean.

Introduction

The presence and availability of nitrogen often limits primary production in the ocean ((Redfield 1958). Ammonium (NH_4^+) and nitrate (NO_3^-) are important inorganic nitrogen sources supporting phytoplankton productivity (Dugdale and Goering 1967, Eppley et al 1969). NH_4^+ cycles rapidly in the ocean, often resulting in very low (e.g. nanomolar) concentrations, and the turnover of NH_4^+ in the upper ocean largely reflects the coupling between its assimilation as a nutrient during organic matter production and its production during organic N degradation (Zehr and Kudela 2011). In contrast, NO_3^- supply to the euphotic zone of the open ocean occurs largely through physical processes, including mixing and upwelling; nitrate concentrations tend to be very low in the upper ocean due to rapid biological consumption, with concentrations increasing sharply into the dimly-lit regions near the base of the euphotic zone (Gruber 2008, Voss et al 2013).

Global change and human activities are reshaping the distribution and inventory of the N pool in the surface ocean. Warming of the upper ocean with coincident intensification of thermal stratification has been hypothesized to have led to an overall decrease in the supply of NO_3^- to the surface ocean (Kamykowski and Zentara 2005), while increased atmospheric deposition may be altering the quantity and types of regional input of N to the surface waters of the North Pacific with consequences for nutrient stoichiometry below the euphotic zone (Kim et al 2014). Together, these types of environmental perturbations may impact the proportional supply of NH_4^+ and NO_3^- supporting phytoplankton productivity, which could lead to cascading effects that reshape phytoplankton community structure (Zehr and Kudela 2011) and impact bacterial carbon processing (Bendtsen et al 2015, Kirchman and Rich 1997) and diversity (Sul et al 2013).

Predicting the effect of changing N source on open ocean nutrient cycling demands that these processes be investigated in the vast oligotrophic gyres that dominate the area of the surface ocean. In the North Pacific Subtropical Gyre (NPSG), persistent stratification and perennially high irradiance foster an upper ocean devoid of inorganic nutrients (Karl and Church 2014), potentially supporting microbial communities that are highly sensitive to shifts in inorganic nutrient availability. Since 1988, the Hawaii Ocean Time-series (HOT) program has conducted near-monthly research cruises to the open ocean field site Station ALOHA (22°45'N, 158°W). Introduction of NO_3^- to the upper ocean in this region occurs through aperiodic to seasonal mixing events and mesoscale vertical entrainment in the lower euphotic zone (Ascani et al 2013, Johnson et al 2010). In contrast, rates of N_2 fixation are elevated in the nutrient-poor but well-lit regions of the upper ocean (Church et al 2009). Thus, the supply and form of nitrogenous nutrients to this ecosystem are both vertically and temporally variable (Karl et al 2008), but little is known of how changes in phytoplankton inorganic N source may alter the quantity, quality, and composition of DOM produced and how it is metabolized *in situ.*

In oceanic gyres, phytoplankton primary production is dominated by the picocyanobacteria *Prochlorococcus* and *Synechococcus* (Li 1994), with the former contributing significantly to global photosynthetic biomass (DuRand et al 2001). Although various strains of *Prochlorococcus* appear unable to assimilate NO_3^-, relying instead on NH_4^+, nitrite, and organic N (Rocap et al 2003), recent field- (Martiny et al 2009) and culture-based (Berube et al 2015) work has demonstrated that the capacity for both *Prochlorococcus* and *Synechococcus* to assimilate and utilize both NH_4^+ and NO_3^- is widespread, though perhaps with reduced assimilation efficiency for the latter (Collier et al 2012, Moore et al 2002). Taken together, these observations emphasize that N sources may alter both the productivity and community structure

Wiley-Blackwell and Society for Applied Microbiology

of NPSG phytoplankton communities, but we have little understanding of how this may impact bacterioplankton growth on *in situ* DOM production.

A significant proportion of primary production is released as dissolved organic matter (DOM) and is subsequently metabolized by osmotrophs (Williams 2000), primarily Bacteria and Archaea, but also eukaryotes including coccolithophores and diatoms (Kujawinski et al 2011). The oceanic DOM pool is the largest pool of reduced carbon (C) (662±32 pg C) in the ocean (Hansell et al 2009) and is extremely diverse in chemical composition and structure (Repeta 2015). DOM composition and reactivity varies in time and space (Hansell 2013) and can be a function of the DOM source (Becker et al 2014, Nelson and Carlson 2012, Wear et al 2015) and the extent of alteration by heterotrophic and abiotic processes (Carlson and Hansell 2015, Kujawinski 2011). How nutrient availability affects the production and consumption of DOM is a key area of current research (Carlson and Hansell 2015).

The goal of the present study was to provide a snapshot example of how abrupt changes in the availability of different forms of N were processed through the intact planktonic community and how the net-DOM produced was subsequently metabolized by bacterioplankton. We sought to explicitly parse the DOM and microbial community response to nutrient enrichment by contrasting whole community responses (unfiltered light incubations in which production and consumption dynamics are coupled and indistinguishable) and heterotrophic microbial responses (dark remineralization incubations in which we can directly associate DOM consumption and transformation to microbial biomass increases, C flux and associated community structure shifts). While many studies have examined how nutrient amendments can alter microbial community production and composition, we have yet to specifically parse the first

crucial trophic transfer in the microbial loop from DOM to bacterioplankton in the context of a nutrient enrichment study.

To accomplish this we conducted an inorganic N addition (NH_4^+ and NO_3^-) experiment with unfiltered surface seawater from Station ALOHA to assess how different inorganic N sources affect photosynthesis, DOM production and microbial community composition over a 10 day simulated phytoplankton bloom. We then sterile-filtered and inoculated the harvested DOM with natural microbial assemblages to examine the subsequent metabolism of DOM, heterotrophic bacterioplankton growth and community compositional responses over a 1-week incubation in the dark (a subsequent 1.5 month incubation was used to assess long-term DOM lability). We hypothesized that the two N sources would differentially stimulate net DOM production and alter the composition of both the microbial community and the DOM produced relative to an unamended control. We further hypothesized that differences in DOM composition induced by N enrichment would translate to differences in lability and impacts on microbial community structure and growth efficiency during additional dark remineralization periods.

Methods

Experimental design

In June 2014, seawater was collected from 5 m depth at Station ALOHA (22.75ºN, 158.00ºW) in the NPSG aboard the *R/V Ka'imikai-O-Kanaloa* using 12 L PVC sampling bottles and subsequently subsampled into 20 L polycarbonate (PC) carboys (Nalgene, Rochester, NY, USA) placed in a shaded on-deck flowing seawater incubator until transport to the shore-based laboratory (~16 h). At the lab, duplicate carboys were amended with N as either KNO_3 (~1.5 μmol L^{-1}; Thermofisher, Waltham, MA, USA) or NH_4Cl (~3.3 μmol L^{-1}; Thermofisher,

Waltham, MA, USA); amendments enriched each inorganic source by ~100-fold relative to ambient levels in the surface waters of Station ALOHA (starting control concentrations were 0.01 μmol L^{-1} and 0.03 μmol L^{-1} for NO_3^- and NH_4^+, respectively). Enrichments were designed to be in excess and approximate the mean inorganic nitrogen levels observed near the base of the euphotic zone (150-200 m NO_3^- at Station ALOHA is typically 1.5 - 3 μmol L^{-1}). We expected that by inducing a phytoplankton bloom these amendment concentrations would afford us the ability to detect measureable changes in TOC concentrations and DOM composition due to production and removal processes. Two additional 20 L carboys handled identically were maintained as unamended controls. Carboys were submerged in a recirculating temperature-controlled (25±1 ºC) rooftop incubator shaded with blue plexiglass sheeting (Altuglas International, Bristol, PA, USA #2069; 25-30% incident irradiance comparable to light flux near the bottom of the surface mixed layer at the time the water was collected). Carboys were incubated for 10 days and sampled daily for concentrations of inorganic nutrients, total organic carbon, bacterioplankton and chlorophyll *a* (chl *a*), as well as fluorescent DOM composition and rates of primary production (estimated using ^{14}C-bicarbonate assimilation).

Seawater dilution and DOM degradation experiments were then conducted using the DOM produced from the grow-out experiment. When chl *a* concentrations were near maximal (10 days), seawater from each carboy was gravity filtered through a pre-flushed (~2 L of Barnsted™ Nanopure™ water; Thermofisher) 142 mm, 0.2 μm filter (Supor®, Pall-Gelman, Port Washington, NY, USA) housed in a PC filter holder (Geotech, Denver, CO, USA) and collected in a separate 10 L PC carboy. Unfiltered and unamended near-surface seawater from Station ALOHA was then used to inoculate the filtrate to a final concentration of 20% v/v. The carboys

were placed in a dark temperature-controlled (25ºC) incubator and sampled daily for ~1 week (6 days). To assess removal and alteration of the semi-labile DOM produced during the grow-out phase of the experiment, the carboys were incubated an additional 43 days (total 49 d) and sampled for all previous parameters excepting chlorophyll concentrations and carbon fixation rates. All carboys and tubing were cleaned with 10% HCl and Nanopure™ water and rinsed with sample water prior to filling.

Sample Collection and Analysis

Inorganic and organic nutrient samples were collected in high-density polyethylene (HDPE) bottles (VWR, Arlington, IL, USA) and stored in an organic-free freezer (-20ºC) until analysis. NO_3^-, silicate and soluble reactive phosphorus (SRP) were analyzed using a segmented flow Seal (AA3) autoanalyzer (Seal Analytical, Mequon, WI, USA) according to Strickland and Parsons (1968) using 5-point standard curve and blank correction to calculate concentrations. NH_4^+ concentrations were measured using indo-phenol blue chemistry and a 2 m liquid waveguide detector (Li et al 2005). Concentrations of total organic carbon (TOC) were analyzed via high temperature combustion using a Shimadzu TOC-V (Shimadzu, Columbia, MD, USA) according to Carlson et al (2010) using a 4-point potassium hydrogen phthalate standard curve. Deep seawater reference material (DSRM) from the Consensus Reference Materials project (Dennis Hansell, University of Miami, FL) were used to assess instrument performance, and references were always within the acceptable range (41-44 µmol C L^{-1}; coefficient of variation 2-3%). Fluorescent DOM was analyzed according to (Nelson et al 2015) using an Aqualog scanning fluorometer (Horiba Scientific, Edison, NJ, USA). We used Parallel Factor Analysis (PARAFAC) to derive and validate three modeled fDOM components with the DOMFluor

toolbox (v1.7; (Stedmon and Bro 2008). PARAFAC analysis identified three spectral components among samples that varied significantly as a function of excitation (Ex) and emission (Em) maxima. These fluorescence regions included the tyrosine-like Peak B (Ex_{max} = 275 nm, Em_{max} = 310 nm, Secondary Em_{max} = 480), the visible humic Peak M (Ex_{max} = 312 nm, Em_{max} = 380-420 nm) and the UV humic Peak A (Ex_{max} = 260 nm, Em_{max} = 380-460 nm) (Coble 1996). The TOC and fDOM samples were not filtered in order to minimize contamination.

Samples for analyses of chl *a* concentrations were collected in 250 ml amber HDPE bottles, filtered onto 25 mm glass fiber filters (GF/F, Whatman™; GE Healthcare and Lifesciences, Pittsburgh, PA, USA); filters were frozen and extracted in 100% HPLC-grade acetone (ThermoFisher) for 24 hrs at -20ºC prior to analysis of the extracts with a 10-AU fluorometer (Turner Designs, Sunnyvale, CA, USA). C fixation rates (1 per treatment bottle) were conducted in acid-cleaned (10% HCl) 250 mL clear PC bottles. ^{14}C-bicarbonate (MP Biochemicals #17441H; Santa Ana, CA, USA) was added to each bottle for a final activity of ~100 μCi L^{-1} and bottles were incubated over the full photoperiod (dawn to dusk), filtered through 25 mm glass fiber filters (Whatman G/FF), acidified with 2N HCl and vented for 24 h in a fume hood. Liquid scintillation counting and determination of ^{14}C specific activities followed the protocol of (Karl et al 1998). Concentrations of chl *a* and C fixation rates were not measured during the dark remineralization experiment.

Samples for subsequent analysis of bacterial abundance were collected daily and analyzed on an Attune Acoustic Focusing Cytometer with Autosampler Attachment (Life Technologies, Eugene, OR, USA) after 1X SYBR Green I staining (Promega, Madison, WI, USA) according to Nelson

et al (2015). Briefly, 2 mL of unfiltered seawater was fixed to 0.5% paraformaldehyde (Electron Microscopy Sciences, Hatfield, PA, USA) in 2 ml polypropylene cryovials, inverted repeatedly to mix, flash frozen in liquid N (LN_2), and then stored at -80ºC. Bacterial biomass was converted to carbon units using a 10 fg C $cell^{-1}$ carbon conversion factor (Christian and Karl, 1994). Samples for planktonic DNA were collected in PC bottles and filtered (~1 L) using a peristaltic pump onto 25 mm, 0.2 µm Supor polyethersulfone filters (Pall). Filters were transferred into 1.5 mL microcentrifuge tubes filled with 400 µL of AP2 lysis buffer (DNeasy Plant Mini Kit, Qiagen, Germantown, MD, USA) and were flash-frozen in liquid N_2 prior to storage at -80ºC. Genomic DNA was extracted from filters after chemical and physical lysis (bead-beating step using both 0.1 and 0.5 mm beads) using the DNeasy Plant Mini Kit following a modified protocol (Paerl et al 2008). The V4 region of the 16S rRNA gene was PCR amplified using the oligonucleotide primer pair F515/R806 with 12 base multiplexing barcodes (Caporaso et al 2011). Paired-end sequencing (250 bp) of the PCR products was performed on an Illumina MiSeq at the Hawaii Institute of Marine Biology Genetics Core Facility (Kaneohe, HI) using the sequencing primers developed by Caporaso et al (2012).

Bioinformatic analyses of 16S DNA amplicon sequences

Mothur software was used for initial demultiplexing, paired-read contig construction and quality screening (Schloss 2009). Briefly, contig consensus construction was done using default settings and sequences were dereplicated to a subset of unique sequences, aligned to the SILVA database (Prüsse et al 2011) and further dereplicated using mothur pre-cluster allowing 2 nucleotide differences (Huse et al 2010); contigs were removed if they had ambiguous bases, >10 nucleotide homopolymers, >1 index mismatch or with lengths outside the expected range 250-

275 nucleotides. Potentially chimeric contigs (Edgar et al 2011) or those classified as plastids, mitochondria, unknown or Eukarya were removed from subsequent analysis. Sequence classification and operational taxonomic unit assignment was done using the software package pplacer (Matsen et al 2010). Sequences were subsampled randomly to 20,000 sequences per sample and aligned using hmmer3 (Eddy 2011) to a modified version of the SILVA v115 SSU database (Pruesse et al 2007, Quast et al 2013). Our database (~53 000 sequences) is an approximation of the SILVA "SEED" subset of hand-curated high quality aligned 16S sequences designed starting with a subset of the SILVA non-redundant reference database (RefNR99 v115) with perfect alignment (alignment quality = 100 in the SSUParc quality database) dereplicated at the 97% sequence identity level with usearch7 (Edgar 2010). This subset was supplemented with sequences that 1) are type strains (*Candidatus* status or SILVA codes [T] s[C] c[S]), 2) are included in the Living Tree Project (Munoz et al 2011, Yarza et al 2008) and 3) have the highest alignment score from any taxonomic classification in SILVA without representation in the previous sequence sets. Common gaps in the alignment were removed, and a maximum likelihood phylogeny was constructed using FastTree (Price et al 2010) using the LTP115 as a constraint tree, the generalized time reversible model of nucleotide evolution and the CAT model of evolutionary rate heterogeneity (Stamatakis 2006). This alignment, taxonomy and phylogenetic tree were compiled into a reference package for pplacer using the pplacer taxtastic toolbox. Phylogenetic placement via pplacer was used for probabilistic assignment of each query sequence to a set of tree edges ranked according to maximum likelihood weight ratio; we also used the highest ranked edge on the SILVA tree and most recent common ancestor classification as an operational taxon (nodal taxonomic unit: NTU) (Vergin et al 2013). From this placement, we calculate metrics of phylogenetic distance among samples (Unifrac and Kantorovich-

Rubinstein distances), phylogenetic diversity (Chao et al 2010, Faith 1992) and NTU or most recent common ancestor taxon relative abundances. Joined, quality-filtered fastq files have been deposited in the NCBI's Sequence Read Archive accession SRP10793.

Because of biases inherent in all PCR primers we present community shifts relative to controls rather than absolute quantification of taxon abundance in communities. Many of the oligotrophic clades that responded directly to N enrichment have been shown using mock communities to be overrepresented by the PCR primers used here, including the NS5 and NS9 clades of Flavobacteria, the OM1/OCS155 clade of Actinobacteria, and the SAR86 and SAR92 clades of Gammaproteobacteria (Parada et al 2015); these primers also underrepresent *Prochlorococcus*, SAR11 and Marine Group I Thaumarchaea (Apprill et al 2015, Parada et al 2015). A complete analysis of the relative abundances and statistical differences in individual NTUs among treatments is provided in the Supplementary Information (Supplementary Table 1); in the results we focus on general phylogenetic patterns.

Statistics and calculations

All statistical analyses were conducted using JMP 11 (SAS, Cary, NC, USA). Hierarchical clustering using Ward's minimum variance method was performed to group samples according to microbial taxon relative abundance and/or fDOM composition. Prior to clustering, data were transformed to approximate Gaussian (normal) distributions and standardized by subtracting the variable mean and dividing by the variable standard deviation to avoid weighting parameters by the absolute measurement values. Analysis of variance (ANOVA) and Tukey and Dunnett's *post hoc* tests were used to determine significant differences among treatments or of treatments relative to the control, respectively. For microbial community structure data, NTUs were

Wiley-Blackwell and Society for Applied Microbiology

considered to have changed significantly in experiments if $\log_2$ ratio (treatment:control) was greater than 1, relative abundance in the treatment group was greater than 0.01% (more than an average of 2 sequences per sample) and FDR-corrected *p*-values from Dunnet's test were less than 0.05 to minimize Type 1 error rates (Benjamini and Hochberg 1995).

Bacterial specific growth rates in the N addition and DOM remineralization experiments were calculated as the natural log of biomass over the logarithmic growth phase (over 3-6 days and 0.5-4 days, respectively). Bacterial growth efficiency (BGE) in the remineralization experiment was calculated as the ratio of the rate of bacterial production (BP; change in bacterial biomass over 0-4 days as measured by changes in abundance and applying the bacterial carbon conversion factor of 10 fg C $cell^{-1}$) relative to the rate of bacterial carbon demand (BCD; change in TOC concentration over 6 days). Phytoplankton specific growth rates were calculated as the natural log change in chl *a* concentrations over log-linear growth (5-9 days). The percentage of carbon partitioned into DOM was calculated using a C:chl *a* ratio of 50 g g^{-1} (Campbell et al 1994).

Results

Net community biogeochemical response to nitrogen pulses in the light

Changes in dissolved inorganic and organic nutrients for each of the experimental phases are reported in Table 1. Concentrations of SRP, silicate, NO_3^- and NH_4^+ in the near-surface water at the time of our sampling were ~ 0.10 µmol L^{-1}, 1.2 µmol L^{-1}, 0.015 µmol L^{-1}, and 0.035 µmol L^{-1}, respectively. In the N addition experiment, inorganic N concentrations did not change significantly in the control treatment and nearly all of the added N was utilized by 10 days in the

NO_3^- and NH_4^+ addition treatments, with concomitant consumption of 0.02 and 0.04 μmol L^{-1} SRP and 0.6 to 0.7 μmol L^{-1} silicate (Table 1).

Initial chl *a* concentrations and C fixation rates ranged from 0.14-0.19 μg chl *a* L^{-1} and 0.72-0.83 μmol C L^{-1} d^{-1}, respectively, and were not significantly different across treatments (chl *a* ANOVA: $p = 0.21$; C fixation ANOVA: $p = 0.40$) (Fig. 1a,1b). Small increases in C fixation rates and chl *a* concentrations occurred in the controls over the first 4 days, but both decreased within a few days to near initial levels. In the NO_3^- and NH_4^+ addition treatments, 7- and 11-fold increases in chl *a* concentrations were observed with maxima on day 8 and day 10, respectively (Fig. 1a).

Phytoplankton specific growth rates were significantly greater in the NO_3^- and NH_4^+ treatments relative to the controls (Table 1). A 5- and 8-fold increase in C fixation rates occurred by day 7 and 9 in the NO_3^- and NH_4^+ additions, respectively (Fig. 1b). Time-integrated (10 days) C fixation rates were highest in the NH_4^+-addition (467.2±29.6 μg C L^{-1}; Table 1), but the percentage of C fixation partitioned into net-TOC by day 10 in the N-addition treatments was equivalent (~22%). Initial bacterial cell abundances were ~6 x 10^8 cells L^{-1} in all treatments (Fig. 1c). Significant bacterial growth occurred, and nearly equivalent changes in bacterial C occurred in the NO_3^- and NH_4^+ addition treatments (Fig. 1c; Table 1). Bacterial specific growth rates were significantly higher in the N-addition treatments relative to the controls (Table 1).

Initial TOC concentrations were equivalent across treatments (e.g. 73-76 μmol C L^{-1}) and in ambient seawater (Fig. 1c). Mean net-TOC production (e.g. ΔTOC) was greater in the NO_3^- and NH_4^+ addition treatments by day 10 (ΔTOC = 9.2±2.4 and 11.5±3.8 μmol C L^{-1}, respectively) relative to the controls (ΔTOC = 4.9±1.5 μmol C L^{-1}), but did not differ significantly between treatments (Table 1 and Fig. 1c). DOM composition also shifted in

Wiley-Blackwell and Society for Applied Microbiology

response to the addition of N. Differential production of UV-humic fDOM above the ambient water was detected in all treatments; the largest increases were observed in the NH_4^+ treatments followed by the NO_3^- treatments, and then the control (Fig. 2). Significant visible humic fDOM production occurred only in the NH_4^+ treatments and there was no statistically significant production or removal of tyrosine-like fDOM (Fig. 2).

Heterotrophic biogeochemical response to recently-produced DOM

In the dark remineralization phase of the experiment, there was no detectable TOC drawdown in the controls, but significant TOC removal occurred in the N-treatments (Table 1). Greater TOC removal (e.g. ΔTOC) occurred by day 6 in the NH_4^+ relative to the NO_3^- treatments (-5.9±0.5 and -2.2±0.1 μmol C L^{-1}, respectively) (Table 1 and Fig. 1d). These changes corresponded to 55% and 24% of the additional TOC added above the controls for the NH_4^+ and NO_3^- treatments, respectively. Initial bacterial abundances were equivalent in all treatments (~2.5 x 10^8 cells L^{-1}; Fig. 1c) and abundances doubled in the NO_3^- and NH_4^+ treatments by day 2 and 4, respectively, after which no net increase in cell abundances occurred (Fig. 1d); significantly more bacterial biomass accumulated in the N treatments relative to the controls over the initial 4 days (Table 1). The computed BGE in the N-derived DOM remineralization treatments did not differ significantly and ranged roughly from 0.1 to 0.3; BGE could not be computed for the controls due to negligible change in TOC (Table 1). Initial concentrations of inorganic nutrients did not differ significantly in the dark remineralization experiment from those observed in at the time of sample collection or at day 10 of the grow-out ($p > 0.05$).

Long-term DOM remineralization dynamics

Wiley-Blackwell and Society for Applied Microbiology

By 49 days in the DOM remineralization experiment, changes in TOC concentrations were equivalent between the NH_4^+ and NO_3^- sources (-7.1 ± 2.2 and -6.8 ± 3.8 μmol C L^{-1}, respectively); there was no detectable change in TOC in the controls. DOM composition at 49 days differed significantly from the start of the dark remineralization, indicating long-term heterotrophic production of fDOM. Significant fDOM production in tyrosine-like fDOM relative to the day 0 controls was only observed in the NH_4^+ DOM degradation treatments by day 49, while fDOM production in visible humic-like fDOM was observed in all treatments by day 49, with no significant change in UV humic-like fDOM in any treatment (Fig. 2).

Bacterial and Archaeal community responses to nitrogen enrichment

Across all treatments, samples clustered significantly into 5 main groups with distinct community structure according to phylotype relative abundances (Figure 3); we have annotated the clusters according to the samples in each as: NO_3^--enriched, NH_4^+-enriched, 1-day N-DOM enriched, 1-week N-DOM enriched, and control/ambient seawater samples (Fig. 3). Thus, while inorganic N sources differentially altered community structure in the light, DOM derived from the two different N-amendments induced similar successional patterns during dark remineralization growth. Importantly, both light and dark controls clustered with ambient communities, indicating a significant but small shift away from ambient ocean waters. This sample clustering pattern was highly consistent whether samples were clustered using raw Bray-Curtis distances among all NTUs or Linnaean classification-based phylotypes (Fig. 3), or based solely on phylogenetic distance among samples (Unifrac or Kantorovich-Rubinstein distances; data not shown). All subsequent statistical analyses of NTUs and families were done comparing mean relative abundances among these 5 distinct sample groupings (Fig. 4).

A suite of common oligotrophic oceanic bacterial taxa, including SAR11, SAR116, SAR86 and *Prochlorococcus*, were found in greatest relative abundances in the ambient and control samples (Fig. 3). Oligotrophic surface Archaea (primarily Marine Group II, Halobacteriales) did not change significantly in experiments, and were typically <1% of the total community. Relative to the ambient and control samples, the N-amendment incubations induced significant enrichment of *Synechococcus* and multiple genera of Flavobacteriaceae within the first 5-6 days of the experiment (Figs. 3, 4a, 4b, 4e, 4f). The NO_3^- amendment was enriched in the oligotrophic Gammaproteobacteria SAR86, SAR92 and OM60 and Flavobacteria clades NS5 and NS9 (Figs. 3, 4e, 4n, 4p) while the NH_4^+ amendment community was enriched in multiple genera of Rhodobacteraceae (*Marinovum, Rhodobacter, Paracoccus* and *Roseovarius)* and the widespread oligotrophic Actinobacteria OM1 and Alphaproteobacteria KI89A clades (Figs. 3, 4k, 4o). Relative abundances of SAR11, SAR86 and SAR116 declined in the NH_4^+ treatment relative to the controls. Analysis of 16S plastid NTU composition provided evidence of clear eukaryotic community differentiation among control/ambient, NO_3^-- and NH_4^+-enriched samples (Supplementary Fig. 1)

In the subsequent remineralization phase a suite of copiotrophic taxa were enriched on N-DOM cultures relative to the controls (Fig. 3). Within 1 d of inoculation genera belonging to the Gammaproteobacteria Alteromonadaceae (*Alteromonas, Aestuariibacter, Glaciecola*) and Oceanospirillaceae (*Oleiphilus, Oleispira*) increased significantly in relative abundance in response to N-DOM but not in control incubations (Figs. 4c, 4i, 4j). After ~1 week of incubation N-DOM cultures were dominated by the Alphaproteobacteria Rhodobacteraceae (*Oceanicola, Pseudoruegeria, Palleronia, Pirellula* and the AS-21 clade) and Hyphomonadaceae, with Alteromonadaceae and Oceanospirillaceae remaining significantly enriched throughout the

experiment relative to controls (Figs. 4d, 4g, 4h). We found no clear multivariate community structure differences between mesocosms amended with NO_3^-enriched or $NH4^+$-enriched DOM (Figure 3), suggesting that inorganic N enrichment, regardless of source, has the largest impact on the heterotrophic community utilizing recently-produced DOM.

Discussion

Inorganic N enrichment can alter phytoplankton community structure and production

The 5-10 fold increase in carbon fixation and chl *a* induced by inorganic nitrogen amendment (Figure 1 and Table 1) was similar to the maxima previously observed in blooms induced by mesopelagic nutrient entrainment by mesoscale eddies in subtropical gyres (Benitez-Nelson et al 2007, McGillicuddy et al 2007). Moreover, the addition of either N source shifted photosynthetic bacterial community structure: within one week of N amendment the relative abundances of *Synechococcus* sequences increased from 1% to 3-5% and were significantly enriched in both N amendments relative to controls (Fig. 4f). We do not have direct evaluation of eukaryotic community composition, but analysis of 16S plastid NTU composition showed clear community differentiation of control, NO_3^-- and NH_4^+-enriched samples (Supplementary Fig. 1) and we observed significant drawdown of silicate in the N-addition treatments (Table 1), suggesting net diatom growth likely increased in response to both N additions. Our results suggest that the addition of NH_4^+ increased *Synechococcus* relative abundances to a greater extent than *Prochlorococcus*. Various strains of *Synechococcus* have previously been shown to grow well in the presence of NH_4^+ (Bronk and Ward 1999, Moore et al 2002). While the enhanced relative abundance of *Synechococcus* under NH_4^+ addition may be due to the lower metabolic cost of assimilating NH_4^+ versus NO_3^- (Dortch 1990, Syrett 1981), certain strains can

exhibit near equivalent growth responses to NH_4^+ and NO_3^- (Collier et al 2012) and it is difficult to definitively ascertain from this work. Daily (Wilson et al 2015) to seasonal (Mahaffey et al 2012) variability in phytoplankton community physiological growth state has been demonstrated at Station ALOHA, and this factor likely shaped the response of the phytoplankton community to nutrient enrichment in this study.

Inorganic N source can alter fluorescent dissolved organic matter composition

Our results suggest that differences in inorganic N source can affect the composition of freshly produced fluorescent DOM (Fig. 2), consistent with previous studies that have demonstrated experimental microbial autotrophic and heterotrophic fDOM production (Rochelle-Newall and Fisher 2002, Romera-Castillo et al 2011). Compositional differences in fDOM production may reflect differences in the composition of autotrophic and heterotrophic assemblages selected by the N-additions (Figs. 3 and 4): the two N-addition treatments here appear to alter phytoplankton communities and fDOM within a week, indicating that different phytoplankton assemblages produce different fDOM (consistent with Becker et al (2014) and subsequent bacterial reshaping of freshly produced algal-derived DOM (Romera-Castillo et al 2011, Shimotori et al 2012). Our results also demonstrated that on month-long timescales (49 d), bacterioplankton produced different types of fDOM in the dark as they degraded DOM derived from the different N-fueled treatments (Fig. 2). Bacterioplankton growing on fresh DOM can chemically alter this material relative to its source characteristics, while simultaneously producing new and distinct compounds (Kujawinski 2011, Ogawa et al 2001). Previous research has documented heterotrophic production of fDOM in dark incubations (Nelson et al 2004, Rochelle-Newall and

Fisher 2002, Romera-Castillo et al 2011), and such mechanisms are consistent with observations of fDOM enrichment in deep ocean waters (Jørgensen et al 2011, Yamashita and Tanoue 2008).

Inorganic N sources can alter the short-term lability of DOM produced by phytoplankton

In the dark remineralization experiment, more NH_4^+-derived TOC was utilized by heterotrophic bacterioplankton than NO_3^--derived TOC in the first week, indicating that the short-term lability of DOM can be influenced by N source, likely by altering phytoplankton community structure and the composition of DOM that is subsequently produced. This idea is consistent with previous research demonstrating that the lability timescales (e.g. Romera-Castillo et al 2011) and composition of fresh DOM can vary as a function of phytoplankton species (Biersmith and Benner 1998; Aluwihare and Repeta 1999). Over monthly time scales (i.e. 49 d), similar concentrations of NO_3^-- and NH_4^+-derived TOC were removed, suggesting that the semi-labile DOM fractions produced by the two N-amendments were equivalent in bioavailability, if not composition (discussed above), and that long-term DOM lability is ultimately controlled by heterotrophic bacterial removal rather than autotrophic production processes (Meon and Kirchman 2001). It is important to note that nutrient co-limitation likely did not enhance TOC drawdown in the N-derived DOM remineralization treatments, as there was no excess NH_4^+ or NO_3^- in these experiments and little measurable inorganic nutrient utilization during the dark remineralization phase of the experiment (Table 1). Lastly, we must emphasize that the timing of when DOM is harvested can also affect short-term TOC lability, which can vary throughout different phases of a bloom (Wear et al 2015b).

Inorganic N enrichment can induce shifts in bacterial community composition

Wiley-Blackwell and Society for Applied Microbiology

We observed subtle but significant differences among treatments in microbial communities according to the form of inorganic N added to the incubations. The ambient community comprised taxa that are common to the waters at Station ALOHA (Bryant et al 2015, DeLong et al 2006) and the dominance of these taxa were maintained in the controls throughout both phases of the incubation (Figs. 3 and 4), demonstrating that there was minimal contamination or bottle incubation effects on the community. Moreover, these taxa dominated community structure in all samples (control and N enriched treatments), emphasizing that the induced production of organic matter did not generate a drastic shift in community structure, only subtle (but significant) enrichment of selected taxa. Many of the taxa enriched by nitrogen additions here are consistent with those enriched in natural and nutrient-induced phytoplankton blooms, including widespread observations of Flavobacteria and Roseobacter enrichment (Buchan et al 2014, Teeling et al 2012, Wear et al 2015a, Nelson et al 2014, Landa et al 2016, Shilova et al 2017) but also enrichment in Actinobacteria OM1/OCS155 and Gammaproteobacteria SAR86 as observed in subtropical mesoscale eddies (Nelson et al 2014), enrichment in copiotrophic Alteromonadaceae and Oceanospirillaceae observed in both coastal upwelling blooms (Wear et al 2015a) and subtropical gyre nitrogen additions (Shilova et al 2017), and enrichments in oligotrophic Gammaproteobacterial clades (OM60/NOR5, SAR92, KI89A) variously documented in both upwelling (Wear et al 2015a, Teeling et al 2012) and Southern Ocean iron enrichments (Landa et al 2016). The growth of Flavobacteria under N enrichment may be associated with the stimulation of phytoplankton growth (Fig. 1), as Flavobacteria are widely recognized to capitalize on particulate matter (Crump et al 1999, DeLong et al 1993, Fandino et al 2001, Rath et al 1998), and similar processes may be guiding some of the other taxa enriched. It is especially notable that numerous uncultured oligotrophic

clades responded differentially to NH_4^+ (OM1, KI89A) or NO_3^- (SAR92, OM60, NS5, NS9), emphasizing that there is a complex consortium of slow-growing oligotrophs that may be responsive to abrupt shifts in inorganic nutrient availability and/or secondarily responding to phytoplankton growth. Beier et al (2015) suggest that DOM composition and competition within microbial communities are integral for determining community function, and Landa et al (2016) explore how differences in DOM compositional changes associated with bloom degradation may structure microbial communities and bacterioplankton production. Our results lend support to these studies, and can be coupled with recent parallel work showing direct effects of inorganic and organic N on phytoplankton and heterotrophic bacterial communities (Shilova et al 2017). The subtle response to either nutrient or DOM enrichment demonstrated here underscores the ecological relevance, as specific taxa groups respond to enrichments while the baseline community remains stable relative to the ambient waters. Our results may guide further work toward a more predictive assessment of how microbial communities may change under trends of shifting nutrient availability.

DOM released after N-enrichment alters heterotrophic bacterial community structure

During dark remineralization the rapid (~1 d) growth of gammaproteobacterial copiotrophs in the Alteromonadaceae and Oceanospirillaceae is consistent with previous studies (Lauro et al 2009, Nelson and Carlson 2012, Nelson and Wear 2014, Wear et al. 2015) and supports a view of these copiotrophs as ecologically relevant "first responders" to the availability of labile DOM in the absence of grazing (Pedler et al 2014). Rhodobacteraceae (including members of the widely studied Roseobacter clades) were most enriched on NH_4^+ and ~1 week DOM remineralization, trends that correspond to their perceived role as opportunistic and

relatively slow growing copiotrophs (Nelson and Carlson 2012, Wear et al 2015) that thrive on the products of other microbial consortia (Buchan et al 2014, Luo et al 2012, Nelson and Carlson 2012, Sarmento et al 2013, Wagner-Döbler and Biebl 2006). Notably, the clades of Rhodobacteraceae that were enriched on NH_4^+-amended and N-DOM amendments were different, suggesting some parsing of ecological niche space between inorganic and organic nutrient specialists. In all cases, the changes in amended microbial community structure were markedly different from the controls and ambient waters suggesting that N-stimulated DOM production may result in short and long-term cascading shifts in community structure that may impact food web dynamics and C and energy flow.

Considerations for future work

This experiment details a single example of trends in DOM production, composition and lability and microbial community responses induced by an abrupt shift in N availability. While NO_3^- and NH_4^+ were added in vast excess (roughly 2 orders of magnitude above background) and in different absolute quantities (roughly 1.5 and 3 μmol N l^{-1}, respectively) the majority of biogeochemical responses did not differ between the two treatments, including SRP and silicate drawdown, and primary, bacterial or TOC production. Major differences between the two substrates were observed in bacterioplankton community shifts and subsequent remineralization dynamics, suggesting a qualitative rather than quantitative impact. It is important to reiterate that while the addition of NO_3^- and NH_4^+ in excess concentrations induced a phytoplankton bloom on an ecologically-relevant scale, the excessive and different enrichments cannot be ruled out as one reason for the observed differential effects. Here we have demonstrated the potential for nitrogen enrichment to induce differential DOM production and remineralization so that future studies

Wiley-Blackwell and Society for Applied Microbiology

may consider adding smaller quantities of nutrients to more closely mimic specific oceanographic processes.

A second important caveat of the experiment is the timescales of examination. While the sampling scales of phytoplankton, bacteria and DOM variables clearly captured the relevant temporal dynamics with reasonable resolution, our assessments of microbial community structure may not be representative of the relevant temporal successional dynamics. Perhaps more importantly, the timing of when DOM was "harvested" for the subsequent dark remineralization may be vastly inappropriate: while we captured the DOM during the period of peak chl *a* concentrations, this also allowed a long period of whole community remineralization and internal recycling with the potential for different interpretations of lability if the DOM were harvested earlier or later. Wear et al. (2015) and Nelson and Wear (2014) addressed this issue explicitly, showing the dramatic differences in DOM lability and microbial community response to DOM harvested on hourly to daily scales throughout a naturally progressing bloom; interestingly many of the same organisms were enriched in dark remineralization incubations in that work. Addressing this issue in future experimental studies is vital and should be a priority.

Acknowledgements

We thank Susan Curless and Alexa Nelson for analyses of inorganic nutrients, and acknowledge the efforts of the Hawaii Ocean Time-series staff for their support of this project. We thank Amy Eggers, director of the Evolutionary Genomics Core Facility, Hawai'i Institute of Marine Biology, University of Hawai'i at Mānoa for DNA sequencing. The authors declare no conflict of interest.

References Cited

Aluwihare, L.I. and Repeta, D.J., (1999). A comparison of the chemical characteristics of oceanic DOM and extracellular DOM produced by marine algae. *Mar Ecol Prog Ser*, *186*, pp.105-117.

Apprill A, McNally S, Parsons R, Weber L (2015). Minor revision to V4 region SSU rRNA 806R gene primer greatly increases detection of SAR11 bacterioplankton. *Aquat Microb Ecol* **75:** 129-137.

Ascani F, Richards KJ, Firing E, Grant S, Johnson KS, Jia Y *et al* (2013). Physical and biological controls of nitrate concentrations in the upper subtropical North Pacific Ocean. *Deep Sea Res II* **93:** 119-134.

Becker JW, Berube PM, Follett CL, Waterbury JB, Chisholm SW, DeLong EF *et al* (2014). Closely related phytoplankton species produce similar suites of dissolved organic matter. *Front Microbiol* **5**.

Beier S, Rivers AR, Moran MA, Obernosterer I (2015). The transcriptional response of prokaryotes to phytoplankton-derived dissolved organic matter in seawater. *Environ Microbiol* **17:** 3466-3480.

Bendtsen J, Hilligsøe KM, Hansen JL, Richardson K (2015). Analysis of remineralisation, lability, temperature sensitivity and structural composition of organic matter from the upper ocean. *Prog Oceanogr* **130:** 125-145.

Benitez-Nelson, C. R., R. R. Bidigare, T. D. Dickey, and others. (2007). Mesoscale Eddies Drive Increased Silica Export in the Subtropical Pacific Ocean. Science **316**: 1017–1021. doi:10.1126/science.1136221

Benjamini Y, Hochberg Y (1995). Controlling the false discovery rate: A practical and powerful approach to multiple testing. *Journal of the Royal Statistical Society Series B (Methodological)* **57:** 289-300.

Berube PM, Biller SJ, Kent AG, Berta-Thompson JW, Roggensack SE, Roache-Johnson KH *et al* (2015). Physiology and evolution of nitrate acquisition in *Prochlorococcus*. *ISME J* **9:** 1195-1207.

Biersmith, A. and Benner, R., (1998). Carbohydrates in phytoplankton and freshly produced dissolved organic matter. *Mar Chem*, **63:** 131-144.

Bronk D, Ward B (1999). Gross and net nitrogen uptake and DON release in the euphotic zone of Monterey Bay, California. *Limnol Oceanogr* **44:** 573-585.

Bryant JA, Aylward FO, Eppley JM, Karl DM, Church MJ, DeLong EF (2015). Wind and sunlight shape microbial diversity in surface waters of the North Pacific Subtropical Gyre. *ISME J*.

Buchan A, LeCleir GR, Gulvik CA, González JM (2014). Master recyclers: features and functions of bacteria associated with phytoplankton blooms. *Nat Rev Microbiol* **12:** 686-698.

Campbell L, Nolla HA, Vaulot D (1994). The importance of *Prochlorococcus* to community structure in the central North Pacific Ocean. *Limnol Oceanogr* **39:** 954-961.

Caporaso JG, Lauber CL, Walters WA, Berg-Lyons D, Lozupone CA, Turnbaugh PJ *et al* (2011). Global patterns of 16S rRNA diversity at a depth of millions of sequences per sample. *Proc Natl Acad Sci U S A* **108:** 4516-4522.

Caporaso JG, Lauber CL, Walters WA, Berg-Lyons D, Huntley J, Fierer N *et al* (2012). Ultra-high-throughput microbial community analysis on the Illumina HiSeq and MiSeq platforms. *ISME J* **6:** 1621-1624.

Carlson CA, Hansell DA, Nelson NB, Siegel DA, Smethie WM, Khatiwala S *et al* (2010). Dissolved organic carbon export and subsequent remineralization in the mesopelagic and bathypelagic realms of the North Atlantic basin. *Deep Sea Res II* **57:** 1433-1445.

Carlson CA, Hansell DA (2015). DOM sources, sinks, reactivity, and budgets. In: Hansell DA, Carlson CA (eds). *Biogeochemistry of Marine Dissolved Organic Matter*, II edn. Elsevier: London. pp 66-126.

Chao A, Chiu C-H, Jost L (2010). Phylogenetic diversity measures based on Hill numbers. *Philos Trans R Soc Lond B Biol Sci* **365:** 3599-3609.

Christian, J. R., and D. M. Karl. (1994). Microbial community structure at the U.S.-Joint Global Ocean Flux Study Station ALOHA: Inverse methods for estimating biochemical indicator ratios. *J Geophys Res* **99**: 269–176.

Church MJ, Mahaffey C, Letelier RM, Lukas R, Zehr JP, Karl DM (2009). Physical forcing of nitrogen fixation and diazotroph community structure in the North Pacific subtropical gyre. *Global Biogeochem Cycles* **23:** GB2020.

Coble PG (1996). Characterization of marine and terrestrial DOM in seawater using excitation-emission matrix spectroscopy. *Mar Chem* **51:** 325-346.

Collier JL, Lovindeer R, Xi Y, Radway JC, Armstrong RA (2012). Differences in growth and physiology of marine *Synechococcus* (cyanobacteria) on nitrate versus ammonium are not determined solely by nitrogen source redox state. *J Phycol* **48:** 106-116.

Crump BC, Armbrust EV, Baross JA (1999). Phylogenetic analysis of particle-attached and free-living bacterial communities in the Columbia River, its estuary, and the adjacent coastal ocean. *Appl Environ Microbiol* **65:** 3192-3204.

DeLong EF, Franks DG, Alldredge AL (1993). Phylogenetic diversity of aggregate-attached vs. free-living marine bacterial assemblages. *Limnol Oceanogr* **38:** 924-934.

DeLong EF, Preston CM, Mincer T, Rich V, Hallam SJ, Frigaard N-U *et al* (2006). Community genomics among stratified microbial assemblages in the ocean's interior. *Science* **311:** 496-503.

Determann S, Lobbes JM, Reuter R, Rullkötter J (1998). Ultraviolet fluorescence excitation and emission spectroscopy of marine algae and bacteria. *Mar Chem* **62:** 137-156.

Dore JE, Brum JR, Tupas LM, Karl DM (2002). Seasonal and interannual variability in sources of nitrogen supporting export in the oligotrophic subtropical North Pacific Ocean. *Limnol Oceanogr* **47:** 1595-1607.

Dortch Q (1990). The interaction between ammonium and nitrate uptake in phytoplankton. *Mar Ecol Prog Ser* **61:** 183-201.

Dugdale R, Goering J (1967). Uptake of new and regenerated forms of nitrogen in primary productivity. *Limnol Oceanogr* **12:** 196-206.

DuRand MD, Olson RJ, Chisholm SW (2001). Phytoplankton population dynamics at the Bermuda Atlantic Time-series station in the Sargasso Sea. *Deep Sea Res II* **48:** 1983-2003.

Eddy SR (2011). Accelerated profile HMM searches. *PLoS Comput Biol* **7:** e1002195.

Edgar RC (2010). Search and clustering orders of magnitude faster than BLAST. *Bioinformatics* **26:** 2460-2461.

Edgar RC, Haas BJ, Clemente JC, Quince C, Knight R (2011). UCHIME improves sensitivity and speed of chimera detection. *Bioinformatics* **27:** 2194-2200.

Eppley RW, Rogers JN, McCarthy JJ (1969). Half-saturation constants for uptake of nitrate and ammonium by marine phytoplankton. *Limnol Oceanogr* **14:** 912-920.

Faith DP (1992). Conservation evaluation and phylogenetic diversity. *Biol Conserv* **61:** 1-10.

Fandino LB, Riemann L, Steward GF, Long RA, Azam F (2001). Variations in bacterial community structure during a dinoflagellate bloom analyzed by DGGE and 16S rDNA sequencing. *Aquat Microb Ecol* **23:** 119.

Field CB, Behrenfeld MJ, Randerson JT, Falkowski P (1998). Primary production of the biosphere: integrating terrestrial and oceanic components. *Science* **281:** 237-240.

Fuhrman JA (1981). Influence of method on the apparent size distribution of bacterioplankton cells: epifluorescence microscopy compared to scanning electrong microscopy. *Mar Ecol Prog Ser* **5:** 103-106.

Goldberg SJ, Carlson CA, Hansell DA, Nelson NB, Siegel DA (2009). Temporal dynamics of dissolved combined neutral sugars and the quality of dissolved organic matter in the Northwestern Sargasso Sea. *Deep Sea Res I* **56:** 672-685.

Gruber N (2008). The marine nitrogen cycle: overview and challenges. *Nitrogen in the Marine Environment***:** 1-50.

Hansell DA, Carlson CA, Repeta DJ, Schlitzer R (2009). Dissolved organic matter in the ocean: a controversy stimulates new insights. *Oceanography*.

Hansell DA (2013). Recalcitrant dissolved organic carbon fractions. *Ann Rev Mar Sci* **5:** 421-445.

Huse SM, Welch DM, Morrison HG, Sogin ML (2010). Ironing out the wrinkles in the rare biosphere through improved OTU clustering. *Environ Microbiol* **12:** 1889-1898.

Johnson KS, Riser SC, Karl DM (2010). Nitrate supply from deep to near-surface waters of the North Pacific subtropical gyre. *Nature* **465:** 1062-1065.

Jørgensen L, Stedmon CA, Kragh T, Markager S, Middelboe M, Søndergaard M (2011). Global trends in the fluorescence characteristics and distribution of marine dissolved organic matter. *Mar Chem* **126:** 139-148.

Kamykowski D, Zentara S-J (2005). Changes in world ocean nitrate availability through the 20th century. *Deep Sea Res I* **52:** 1719-1744.

Karl DM, Hebel DV, Björkman K, Letelier RM (1998). The role of dissolved organic matter release in the productivity of the oligotrophic North Pacific Ocean. *Limnol Oceanogr* **43:** 1270-1286.

Karl DM, Bidigare RR, Church MJ, Dore JE, Letelier RM, Mahaffey C *et al* (2008). The nitrogen cycle in the North Pacific trades biome: an evolving paradigm. In: Capone DG, Bronk DA, Mulholland MR, Carpenter EJ (eds). *Nitrogen In the Marine Environment*. Elsevier: The Netherlands. pp 705-769.

Karl DM, Church MJ (2014). Microbial oceanography and the Hawaii Ocean Time-series programme. *Nat Rev Microbiol* **12:** 699-713.

Kim I-N, Lee K, Gruber N, Karl DM, Bullister JL, Yang S *et al* (2014). Increasing anthropogenic nitrogen in the North Pacific Ocean. *Science* **346:** 1102-1106.

Wiley-Blackwell and Society for Applied Microbiology

Kirchman D, Rich J (1997). Regulation of bacterial growth rates by dissolved organic carbon and temperature in the equatorial Pacific Ocean. *Microb Ecol* **33:** 11-20.

Kujawinski EB (2011). The impact of microbial metabolism on marine dissolved organic matter. *Ann Rev Mar Sci* **3:** 567-599.

Landa M, Blain S, Christaki U, Monchy S, Obernosterer I (2016). Shifts in bacterial community composition associated with increased carbon cycling in a mosaic of phytoplankton blooms. *ISME J* **10:** 39-50.

Lauro FM, McDougald D, Thomas T, Williams TJ, Egan S, Rice S *et al* (2009). The genomic basis of trophic strategy in marine bacteria. *Proc Natl Acad Sci U S A* **106:** 15527-15533.

Li QP, Zhang J-Z, Millero FJ, Hansell DA (2005). Continuous colorimetric determination of trace ammonium in seawater with a long-path liquid waveguide capillary cell. *Mar Chem* **96:** 73-85.

Li WK (1994). Primary production of prochlorophytes, cyanobacteria, and eucaryotic ultraphytoplankton: measurements from flow cytometric sorting. *Limnol Oceanogr* **39:** 169-175.

Lindeman RL (1942). The trophic-dynamic aspect of ecology. *Ecology* **23:** 399-417.

Luo H, Löytynoja A, Moran MA (2012). Genome content of uncultivated marine Roseobacters in the surface ocean. *Environ Microbiol* **14:** 41-51.

Mahaffey C, Bjorkman KM, Karl DM (2012). Phytoplankton response to deep seawater nutrient addition in the North Pacific Subtropical Gyre. *Mar Ecol Prog Ser* **460:** 13-34.

Martiny AC, Kathuria S, Berube PM (2009). Widespread metabolic potential for nitrite and nitrate assimilation among *Prochlorococcus* ecotypes. *Proc Natl Acad Sci U S A* **106:** 10787-10792.

Matsen FA, Kodner RB, Armbrust EV (2010). pplacer: linear time maximum-likelihood and Bayesian phylogenetic placement of sequences onto a fixed reference tree. *BMC Bioinformatics* **11:** 538.

McGillicuddy, D. J., L. A. Anderson, N. R. Bates, and others. (2007). Eddy/Wind Interactions Stimulate Extraordinary Mid-Ocean Plankton Blooms. Science **316**: 1021–1026. doi:10.1126/science.1136256

Meon, B. and Kirchman, D.L., (2001). Dynamics and molecular composition of dissolved organic material during experimental phytoplankton blooms. *Mar Chem*, *75*(3), pp.185-199.

Moore LR, Post AF, Rocap G, Chisholm SW (2002). Utilization of different nitrogen sources by the marine cyanobacteria *Prochlorococcus* and *Synechococcus*. *Limnol Oceanogr* **47:** 989-996.

Wiley-Blackwell and Society for Applied Microbiology

Munoz R, Yarza P, Ludwig W, Euzeby J, Amann R, Schleifer K-H *et al* (2011). Release LTPs104 of the All-Species Living Tree. *Syst Appl Microbiol* **34:** 169-170.

Nelson CE, Carlson CA (2012). Tracking differential incorporation of dissolved organic carbon types among diverse lineages of Sargasso Sea bacterioplankton. *Environ Microbiol* **14:** 1500-1516.

Nelson, C. E., C. A. Carlson, C. S. Ewart, and E. R. Halewood. (2014). Community differentiation and population enrichment of Sargasso Sea bacterioplankton in the euphotic zone of a mesoscale mode-water eddy. Environ Microbiol **16**: 871–887. doi:10.1111/1462-2920.12241

Nelson CE, Wear EK (2014). Microbial diversity and the lability of dissolved organic carbon. *Proc Natl Acad Sci U S A* **111:** 7166-7167.

Nelson CE, Donahue MJ, Dulaiova H, Goldberg SJ, La Valle FF, Lubarsky K *et al* (2015). Fluorescent dissolved organic matter as a multivariate biogeochemical tracer of submarine groundwater discharge in coral reef ecosystems. *Mar Chem* **177:** 232-243.

Nelson NB, Carlson CA, Steinberg DK (2004). Production of chromophoric dissolved organic matter by Sargasso Sea microbes. *Mar Chem* **89:** 273-287.

Ogawa H, Amagai Y, Koike I, Kaiser K, Benner R (2001). Production of refractory dissolved organic matter by bacteria. *Science* **292:** 917-920.

Paerl RW, Foster RA, Jenkins BD, Montoya JP, Zehr JP (2008). Phylogenetic diversity of cyanobacterial narB genes from various marine habitats. *Environ Microbiol* **10:** 3377-3387.

Parada AE, Needham DM, Fuhrman JA (2015). Every base matters: assessing small subunit rRNA primers for marine microbiomes with mock communities, time series and global field samples. *Environ Microbiol*.

Pedler BE, Aluwihare LI, Azam F (2014). Single bacterial strain capable of significant contribution to carbon cycling in the surface ocean. *Proc Natl Acad Sci U S A* **111:** 7202-7207.

Price MN, Dehal PS, Arkin AP (2010). FastTree 2 – approximately maximum-likelihood trees for large alignments. *PLoS One* **5:** e9490.

Pruesse E, Quast C, Knittel K, Fuchs BM, Ludwig W, Peplies J *et al* (2007). SILVA: a comprehensive online resource for quality checked and aligned ribosomal RNA sequence data compatible with ARB. *Nucleic Acids Res* **35:** 7188-7196.

Prüsse E, Quast C, Yilmaz P, Ludwig W, Peplies J, Glöckner FO (2011). SILVA: comprehensive databases for quality checked and aligned ribosomal RNA sequence data compatible with ARB. In: Bruijn FJd (ed). *Handbook of Molecular Microbial Ecology I*. John Wiley & Sons, Inc. pp 393-398.

Quast C, Cuboni S, Bader D, Altmann A, Weber P, Arloth J *et al* (2013). Functional coding variants in SLC6A15, a possible risk gene for major depression. *PLoS One* **8:** e68645.

Rath J, Wu KY, Herndl GJ, DeLong EF (1998). High phylogenetic diversity in a marine-snow-associated bacterial assemblage. *Aquat Microb Ecol* **14:** 261-269.

Repeta DJ (2015). Chemical characterization and cycling of dissolved organic matter. In: Hansell DA, Carlson CA (eds). *Biogeochemistry of Marine Dissolved Organic Matter*, II edn. Elsevier: London. pp 22-64.

Rocap G, Larimer FW, Lamerdin J, Malfatti S, Chain P, Ahlgren NA *et al* (2003). Genome divergence in two Prochlorococcus ecotypes reflects oceanic niche differentiation. *Nature* **424:** 1042-1047.

Rochelle-Newall E, Fisher T (2002). Production of chromophoric dissolved organic matter fluorescence in marine and estuarine environments: an investigation into the role of phytoplankton. *Mar Chem* **77:** 7-21.

Romera-Castillo C, Sarmento H, Álvarez-Salgado XA, Gasol JM, Marrasé C (2011). Net production and consumption of fluorescent colored dissolved organic matter by natural bacterial assemblages growing on marine phytoplankton exudates. *Appl Environ Microbiol* **77:** 7490-7498.

Sarmento H, Romera-Castillo C, Lindh M, Pinhassi J, Sala MM, Gasol JM *et al* (2013). Phytoplankton species-specific release of dissolved free amino acids and their selective consumption by bacteria. *Limnol Oceanogr* **58:** 1123-1135.

Schloss PD (2009). A high-throughput DNA sequence aligner for microbial ecology studies. *PLoS One* **4:** e8230.

Shimotori K, Watanabe K, Hama T (2012). Fluorescence characteristics of humic-like fluorescent dissolved organic matter produced by various taxa of marine bacteria. *Aquat Microb Ecol* **65:** 249-260.

Shilova, IN, Mills MM, Robidart JC, Turk-Kubo KA, Björkman KM, Kolber Z, Rapp I, van Dijken GL, Church MJ, Arrigo KR, Achterberg EP, Zehr JP (2017). Differential effects of nitrate, ammonium, and urea as N sources for microbial communities in the North Pacific Ocean. *Limnol Oceanogr* in press.

Smith, S. V. (1984). Phosphorus versus nitrogen limitation in the marine environment. *Limnol Oceanogr* **29**: 1149–1160.

Stamatakis, A. Phylogenetic models of rate heterogeneity: a high performance computing perspective. *Parallel and Distributed Processing Symposium, 2006. IPDPS 2006. 20th International*; 2006/04//.

Stedmon CA, Markager S (2005). Resolving the variability in dissolved organic matter fluorescence in a temperate estuary and its catchment using PARAFAC analysis. *Limnol Oceanogr* **50:** 686-697.

Stedmon CA, Bro R (2008). Characterizing dissolved organic matter fluorescence with parallel factor analysis: a tutorial. *Limnol Oceanogr-Meth* **6:** 572-579.

Steinberg DK, Nelson NB, Carlson CA, Prusak AC (2004). Production of chromophoric dissolved organic matter (CDOM) in the open ocean by zooplankton and the colonial cyanobacterium *Trichodesmium* spp. *Mar Ecol Prog Ser* **267:** 45-56.

Strickland JDH, Parsons TR (1968). Inorganic Micronutrients in Sea Water. *A Practial Handbook of Seawater Analysis*. Fish. Res. Board of Can: Ottawa.

Sul WJ, Oliver TA, Ducklow HW, Amaral-Zettler LA, Sogin ML (2013). Marine bacteria exhibit a bipolar distribution. *Proc Natl Acad Sci U S A* **110:** 2342-2347.

Syrett PJ (1981). Nitrogen-metabolism of microalgae. *Can B Fish Aquat Sci***:** 182-210.

Tedetti M, Cuet P, Guigue C, Goutx M (2011). Characterization of dissolved organic matter in a coral reef ecosystem subjected to anthropogenic pressures (La Réunion Island, Indian Ocean) using multi-dimensional fluorescence spectroscopy. *Sci Total Environ* **409:** 2198-2210.

Teeling, H., B. M. Fuchs, D. Becher, and others. (2012). Substrate-Controlled Succession of Marine Bacterioplankton Populations Induced by a Phytoplankton Bloom. *Science* **336**: 608–611. doi:10.1126/science.1218344

Vergin KL, Beszteri B, Monier A, Cameron Thrash J, Temperton B, Treusch AH *et al* (2013). High-resolution SAR11 ecotype dynamics at the Bermuda Atlantic Time-series Study site by phylogenetic placement of pyrosequences. *ISME J* **7:** 1322-1332.

Voss M, Bange HW, Dippner JW, Middelburg JJ, Montoya JP, Ward B (2013). The marine nitrogen cycle: recent discoveries, uncertainties and the potential relevance of climate change. *Philos Trans R Soc Lond B Biol Sci* **368:** 20130121.

Wagner-Döbler I, Biebl H (2006). Environmental biology of the marine Roseobacter lineage. *Annu Rev Microbiol* **60:** 255-280.

Wear, E. K., C. A. Carlson, A. K. James, M. A. Brzezinski, L. A. Windecker, and C. E. Nelson. (2015a). Synchronous shifts in dissolved organic carbon bioavailability and bacterial community responses over the course of an upwelling-driven phytoplankton bloom. *Limnol Oceanogr* **60**: 657–677. doi:10.1002/lno.10042

Wear EK, Carlson CA, Windecker LA, Brzezinski MA (2015b). Roles of diatom nutrient stress and species identity in determining the short-and long-term bioavailability of diatom exudates to bacterioplankton. *Mar Chem* **177:** 335-348.

Williams PJLEB (2000). Heterotrophic bacteria and the dynamics of dissolved organic material. *Microbial Ecology of the Oceans*. Wiley-Liss: NY. pp 153-200.

Wilson ST, Barone B, Ascani F, Bidigare RR, Church MJ, Valle DA *et al* (2015). Short-term variability in euphotic zone biogeochemistry and primary productivity at Station ALOHA: A case study of summer 2012. *Global Biogeochem Cycles* **29:** 1145-1164.

Yamashita Y, Tanoue E (2003). Chemical characterization of protein-like fluorophores in DOM in relation to aromatic amino acids. *Mar Chem* **82:** 255-271.

Yamashita Y, Tanoue E (2008). Production of bio-refractory fluorescent dissolved organic matter in the ocean interior. *Nature Geoscience* **1:** 579-582.

Yamashita Y, Cory RM, Nishioka J, Kuma K, Tanoue E, Jaffé R (2010). Fluorescence characteristics of dissolved organic matter in the deep waters of the Okhotsk Sea and the northwestern North Pacific Ocean. *Deep Sea Research II* **57:** 1478-1485.

Yarza P, Richter M, Peplies J, Euzeby J, Amann R, Schleifer K-H *et al* (2008). The All-Species Living Tree project: A 16S rRNA-based phylogenetic tree of all sequenced type strains. *Syst Appl Microbiol* **31:** 241-250.

Zehr JP, Kudela RM (2011). Nitrogen cycle of the open ocean: from genes to ecosystems. *Ann Rev Mar Sci* **3:** 197-225.

Figure Legends

Figure 1. Plankton and DOM dynamics in response to N enrichment. Panel (a) shows mean chl *a* concentrations (chl *a*; μg L^{-1}) in the N addition experiment. Panel (b) presents carbon fixation rates (μg C L^{-1} d^{-1}) in the N addition experiment. Panels (c) and (d) present mean bacterial cell counts (left y-axis; open symbols; cells L^{-1}) and total organic carbon (TOC) concentrations (right y-axis; closed symbols; μmol L^{-1}) in the N addition experiment (c) and DOM remineralization experiment (d). Whiskers are standard deviation. Hollow block arrows refer to the timepoints DNA was sampled presented in Figure 3.

Figure 2. Mean DOM fluorescence (fDOM) for specific PARAFAC components in both experiments. Panel (a) is a heatmap showing mean levels of each compound through time. Panel (b) shows mean values at the end of each experiment relative to the ambient water. Letters in panel (b) denote ANOVA with Tukey *post hoc* test; means with the same letter do not differ significantly at $\alpha = 0.05$. Units are Raman units of water (RU).

Figure 3. Clustering of samples by microbial community composition, including a heat map of relative enrichment of family or genus level clades. At bottom samples (columns) are annotated by experiment, treatment type, sampling day, and replicate. Samples are hierarchically clustered (top) according to standardized relative abundance of taxa (rows) using Ward's minimum variance method. Clusters are annotated in color at bottom and using colored boxes in the heatmap for visual interpretation. Taxa are clustered (left) and annotated (right) according to relative enrichment patterns among samples; only families that reached 1% of community in at least one sample are shown. Heatmap colors visualize relative enrichment, not abundance: relative abundances (arcsin-square root transformed) are standardized for each taxon by subtracting the column mean and dividing by the column standard deviation; colors represent different abundances for each family.

Figure 4. Microbial taxon-specific response profiles among treatments. At left bacterial taxa (NTUs; symbols) are plotted according to relative abundance (x-axis) and mean fold-change relative to the mean of the control group (y-axis) in each treatment grouping (panels a-d). NTUs from 6 selected families both abundant and significantly enriched in multiple treatments are color coded (legend at bottom). At center the mean relative abundances of these 6 color-coded families among treatments are shown (panels e-j). At right the mean relative abundances of 6 additional clades dominant in ambient waters at Station ALOHA (> 5%) that responded to treatments are compared across treatment groupings (panels k-p). All ANOVAs are significant (FDR $p < 0.05$) and treatments that differ significantly from the controls (Dunnet's $p < 0.05$) are annotated with an asterisk.

Table 1. Changes in nutrients, total organic carbon (TOC), and phytoplankton and bacterial growth dynamics as a function of N source during the light growth (10 day change) and DOM remineralization (6 day change) phases of the experiment. Values in ***bold italic*** differ significantly from the controls (analysis of variance with Dunnet's *post hoc* test, $\alpha = 0.05$). Time-integrated carbon fixation: primary production (PP); Bacterial specific growth rate: bSGR; phytoplankton specific growth rate: pSGR; bacterial growth efficiency: BGE, calculated as the ratio of bacterial carbon production to bacterial carbon demand. ND stands for not detected when the mean does not differ significantly from zero. N/A stands for not applicable where metrics could not be calculated. pSGR and BGE could not be calculated (NC) for the controls because of insufficiently resolved change in chlorophyll and TOC, respectively.

		N-Amendment – 10 day change			Remineralization – 6 day change		
Metric	**Units**	**Control**	**NO_3^-**	**NH_4^+**	**Control**	**NO_3^-**	**NH_4^+**
ΔNO_3^-	µmol L^{-1}	ND	***-1.53 ± 0.14***	ND	0.004±0.002	ND	ND
ΔNH_4^+	µmol L^{-1}	0.03 ± 0.00	0.07 ± 0.00	***-3.18 ± 0.03***	ND	ND	ND
ΔSRP	µmol L^{-1}	ND	***-0.04 ± 0.01***	***-0.02 ± 0.01***	ND	ND	ND
ΔSilicate	µmol L^{-1}	ND	***-0.58 ± 0.06***	***-0.68 ± 0.08***	0.04 ± 0.01	ND	ND
ΔTOC	µmol L^{-1}	4.9 ± 1.5	***9.2 ± 2.4***	***11.5 ± 3.8***	ND	***-2.2 ± 0.1***	***-5.9 ± 0.5***
ΔBact.C	µmol L^{-1}	0.20 ± 0.10	***0.86 ± 0.07***	***0.82 ± 0.12***	0.01 ± 0.00	***0.12 ± 0.02***	***0.18 ± 0.02***
bSGR	d^{-1}	0.10 ± 0.05	***0.23 ± 0.02***	***0.30 ± 0.05***	0.02 ± 0.01	***0.13 ± 0.04***	***0.23 ± 0.02***
pSGR	d^{-1}	NC	***0.06 ± 0.01***	***0.14 ± 0.01***	N/A	N/A	N/A
PP	µg C L^{-1}	112 ± 6.1	***348 ± 9.6***	***467 ± 30***	N/A	N/A	N/A
BGE		N/A	N/A	N/A	NC	***0.25 ± 0.07***	***0.15 ± 0.04***

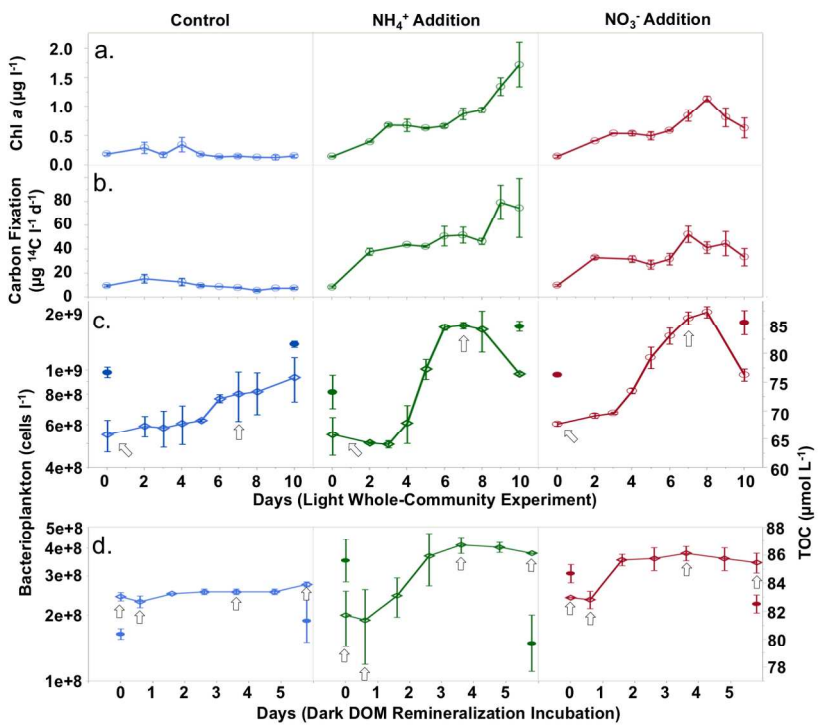

Figure 1. Plankton and DOM dynamics in response to N enrichment. Panel (a) shows mean chl a concentrations (chl a; µg L-1) in the N addition experiment. Panel (b) presents carbon fixation rates (µg C L-1 d-1) in the N addition experiment. Panels (c) and (d) present mean bacterial cell counts (left y-axis; open symbols; cells L-1) and total organic carbon (TOC) concentrations (right y-axis; closed symbols; µmol L-1) in the N addition experiment (c) and DOM remineralization experiment (d). Whiskers are standard deviation. Hollow block arrows refer to the timepoints DNA was sampled presented in Figure 3.

748x561mm (72 x 72 DPI)

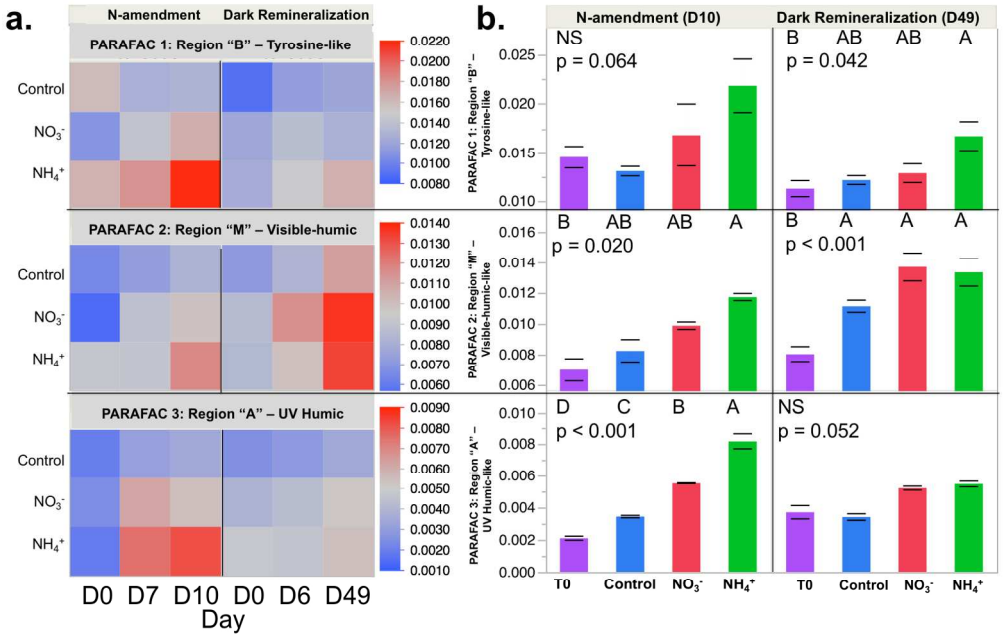

Figure 2. Mean DOM fluorescence (fDOM) for specific PARAFAC components in both experiments. Panel (a) is a heatmap showing mean levels of each compound through time. Panel (b) shows mean values at the end of each experiment relative to the ambient water. Letters in Panel (b) denote ANOVA with Tukey post hoc test; means with the same letter do not differ significantly at α = 0.05. Units are raman units of water (RU).

793x595mm (72 x 72 DPI)

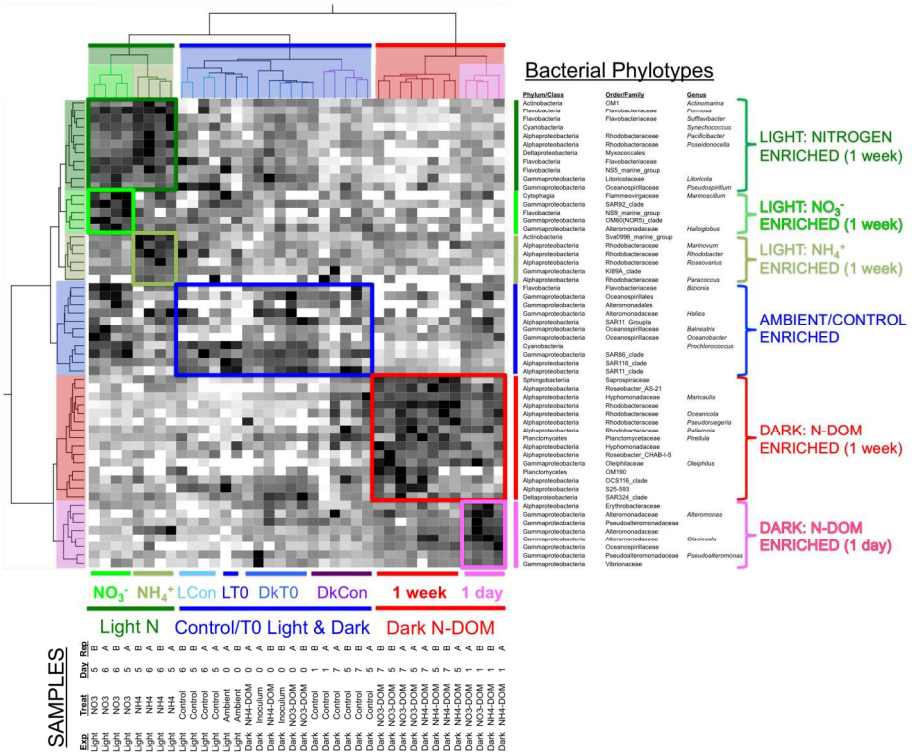

Figure 3. Clustering of samples by microbial community composition, including a heat map of relative enrichment of family or genus level clades. At bottom samples (columns) are annotated by experiment, treatment type, sampling day, and replicate. Samples are hierarchically clustered (top) according to standardized relative abundance of taxa (rows) using Ward's minimum variance method. Clusters are annotated in color at bottom and using colored boxes in the heatmap for visual interpretation. Taxa are clustered (left) and annotated (right) according to relative enrichment patterns among samples; only families that reached 1% of community in at least one sample are shown. Heatmap colors visualize relative enrichment, not abundance: relative abundances (arcsin-square root transformed) are standardized for each taxon by subtracting the column mean and dividing by the column standard deviation; colors represent different abundances for each family.

793x595mm (72 x 72 DPI)

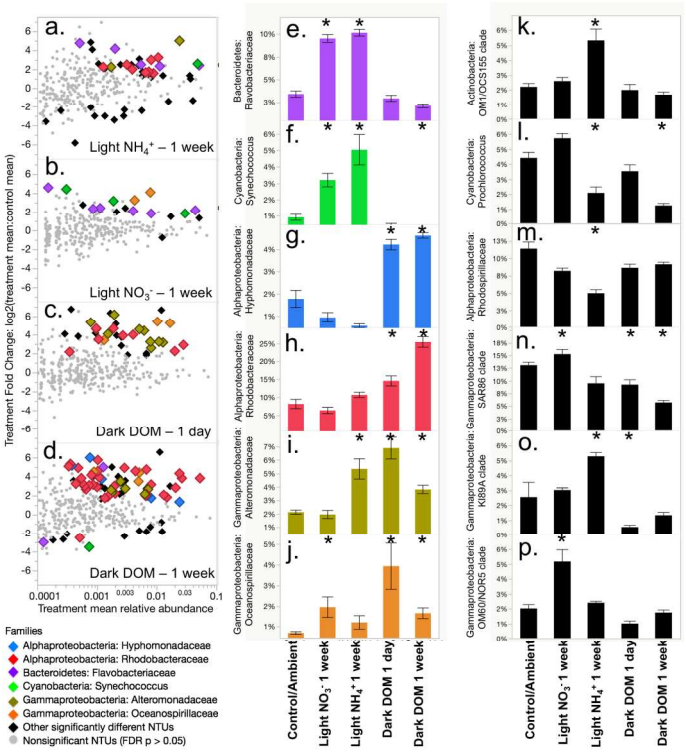

Figure 4. Microbial taxon-specific response profiles among treatments. At left NTUs (symbols) are plotted according to relative abundance (x-axis) and mean fold-change relative to the mean of the control group (y-axis) in each treatment grouping (panels a-d). NTUs from 6 selected families both abundant and significantly enriched in multiple treatments are color coded (legend at bottom). At center the mean relative abundances of these 6 color-coded families among treatments are shown (panels e-j). At right the mean relative abundances of 6 additional clades dominant in ambient waters at Station ALOHA (> 5%) that responded to treatments are compared across treatment groupings (panels k-p). All ANOVAs are significant (FDR $p < 0.05$) and treatments that differ significantly from the Controls (Dunnet's $p < 0.05$) are annotated with an asterisk.

793x595mm (72 x 72 DPI)